

The Effects of Titanium Dioxide (TiO₂) and Reduced Graphene Oxide (rGO) Doping Ratio Variation to the Performance of Dye Sensitized Solar Cell (DSSC)

Afiqah Baharin¹, Siti Kudnie Sahari¹, Rafidah Kemat¹ and Najwa Ezira Ahmed Azhar²

¹Faculty of Engineering, Universiti Malaysia Sarawak (UNIMAS), 94300 Kota Samarahan, Sarawak.

²NANO-SciTech (NST), Institute of Science, Universiti Teknologi MARA (UiTM), 40450 Shah Alam, Selangor.

ABSTRACT

The Titanium Dioxide (TiO₂)-reduced Graphene Oxide (rGO) were synthesized and doped at different concentration of 0.1wt%, 0.3wt% and 0.5wt% by varying the amount of rGO solution. The TiO₂ nanoparticles was prepared via precipitation peptization method while rGO solution was prepared via chemical reduction and deposited by using Doctor Blade technique. The TiO₂-rGO thin films samples were characterized by X-ray Diffraction spectroscopy (XRD) and Ultraviolet-visible spectroscopy (UV-Vis) for structural and optical properties while electrical properties was characterized by Keithley sourcemeter. It is observed that all of the TiO₂-rGO samples possess the anatase TiO₂ crystallinity phase which strongly appeared at (101), (004), (200) and (105) peaks and as the amount of rGO increases, the intensity of the peaks are decreasing. Meanwhile, 0.1wt% of TiO₂-rGO has the highest absorbance wavelength with the lowest band gap at 2.75 eV which due to formation of Ti-O-C bond. These were confirmed by the efficiency obtained by the 0.1wt% of TiO₂-rGO at 1.21% which higher than pure TiO₂. The results obtained confirmed that the properties of TiO₂-rGO and performances of DSSC were affected by the doping ratio.

Keywords: Chemical reduction, Doped, Precipitation-peptization, Reduced Graphene Oxide, Titanium Dioxide.

1. INTRODUCTION

Recently, there are strong interest in the third generation of photovoltaic solar cell technology, especially the Dye Sensitized Solar Cell (DSSC) device. This is due to several benefits of their energy conversion, flexibility, cheap and easy to fabricate as compared to silicon based solar cells [1,2]. DSSC has a sandwich configuration consisting of photoanode, electrolyte, dye and counter electrode [3,4]. There are many work have been done in order to increase the performance of DSSC which include developing of new sensitizers, different counter electrode and photoanode. The photoanode has derived great attention due to its function to transport photo-induced electrons and absorb dye which helps to determine the photo-current density [5].

Among various semiconductor, TiO₂ has been widely used as photoanode in DSSC. This is due to its higher photoactivity, wide band gap of 3.2 eV, low cost and relative non-toxicity [5]. The TiO₂ photoanode has a main role throughout the conversion of light energy to electrical in DSSC. The excited electrons will flow across the Fluorine doped Tin Oxide (FTO), external load and finally to the counter electrode [6]. However, the charge recombination is the main factor that limits the performance of DSSC [7]. This is to say that the back-electron transfer in TiO₂ photoanode-electrolyte interface before reaching the FTO is considered to be the major recombination pathway, which decrease the performance of

*Corresponding author: afiqahb94@gmail.com

DSSC [8]. This problem can be solved including the use of composite semiconductor photoanode with different band gaps and some doping elements in TiO₂ photoanode [6]. In the past two decades, carbon nanotubes (CNTs) and graphene sheets have doped with TiO₂ photoanode to increase the performance of DSSC [9]. The graphene may be more suitable than CNTs for charge separation due to its large surface area, high electron mobility (15000 cm²/V/s), good contact with metal oxides [10]. Therefore, rGO is the potential candidate to be coupled with TiO₂ as photoanode in DSSC since graphene has zero band gap [11]. It helps to generate the electron and hole pairs (EHPs) for high conversion efficient, lengthy visible light absorption and increase the performance of DSSC. In this present work, TiO₂ doped rGO was prepared with different weightage which are 0.1wt%, 0.3wt% and 0.5wt%. The N719 dye will be used as sensitizers. The annealing temperature for the thin film is fixed at 450°C.

2. EXPERIMENTAL METHODS

2.1 Materials

The chemical used during the experiment were Titanium (IV) Isopropoxide (TTIP), propanol (C₃H₈O) and dimethylformamide (DMF) supplied by Sigma Aldrich. Graphene oxide (GO) and Triton X-100 were purchased from R&M Chemicals whereas acetic acid and absolute ethanol were from Fisher Scientific. The chemicals were used without any further purification and entire chemicals were analytical reagents (AR).

2.2 Synthesis of TiO₂

TiO₂ were synthesized via method of precipitation-peptization utilizing Titanium (IV) Isopropoxide (TTIP) as the precursor. Firstly, beaker A was prepared by adding 10 mL of TTIP into 40 mL of propanol. Then, the solution was continuously stirred for 30 minutes at room temperature. In the beaker B, 5 mL of acetic acid, 10 mL of propanol and 100 µL of Triton X-100 were added into 10 mL deionized water. After that, the solution was stirred continuously for 30 minutes at room temperature. Next, the solution in beaker A was added slowly into beaker B with 1 mL/min rate based on previous research [1]. Lastly, the mixture solution was heated on a hot plate at 60°C and stirred at 600 rpm for two hours then left to cool down overnight to surmount the bubbles in the solution.

2.3 Synthesis of rGO

RGO solution was prepared via chemical reduction with graphene oxide (GO) as precursor and hydrazine hydrate as reduction agent. Initially, 2 mL of GO was added into 100 mL of deionized water and sonicated for 10 minutes. Then, the solution was transferred into round bottom conical flask and synthesized by using reflux method in oil bath. After that, 17 µL of hydrazine hydrate was immediately added into the GO solution as soon as heating started. The solution was then stirred on the hot plate at 80°C with 300 rpm stirring speed for 12 hours resulting black color liquid. To acquire the rGO powder, the solution was filtered by using filter membrane to remove the excess water and left to dry for another 12 hours. Next, 40 mL of dimethylformamide (DMF) which act as the solvent was added to 1.5 gram of rGO powder to form rGO solution. Lastly, the solution was sonicated for 15 minutes until entire rGO powder were fully dissolved in DMF.

2.4 Preparation of TiO₂ doped rGO

TiO₂ was doped with different volumes of rGO and the doping weightage were set at 0.1wt%, 0.3wt% and 0.5wt%. For 0.1wt% TiO₂-rGO, 6 mL of rGO solution was mixed with 60 mL of TiO₂ solution in a beaker and stirred continuously for 15 minutes. The steps are repeated for both 0.3wt% and 0.5wt% TiO₂-rGO with different volume of rGO as depicted in Table 1.

Table 1 Volume of TiO₂ and rGO

TiO ₂ -rGO (wt%)	Volume of TiO ₂ (mL)	Volume of rGO (mL)
0.1	60	6
0.3	60	18
0.5	60	30

Next, the mixture was heated on the hot plate at 100°C for 3 hours [1]. Once the powder was fully dried, the powder was annealed at 450°C for 2 hours in the furnace. Then, 100 µL of deionized water was mixed with the TiO₂-rGO powder to form a paste. After that, the paste was deposited on the conductive side of FTO glass by using Doctor Blade method.

2.5 Fabrication of DSSC

The anode and cathode were prepared in order to fabricate DSSC. The FTO substrate coated with 0.1wt% TiO₂-rGO acts as cathode while the substrate coated with graphite acts as anode. For the dye preparation, N-719 dye was mixed with 25mL of absolute ethanol. The substrates were soaked in the dye solution and left overnight to allow the dye to be absorbed by the sample surface. Then, both of the substrates were combined together with a binder clip as shown in Figure 1. A few drops of electrolyte which is Potassium Iodide (KI) were injected between the substrates. The electrical characterization was analysed immediately after the fabrication were done.

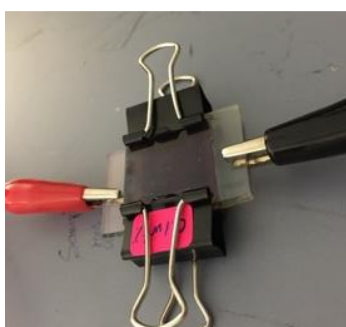


Figure 1. DSSC device

2.6 Characterization

The X-ray diffraction spectroscopy (XRD, PANalytical X'PERT PRO MRD PW 3040) was used to determine the phase structure of a crystalline material in TiO₂-rGO. The scanning rate employed was 0.033°s⁻¹ in 2θ range from 20° to 80° with Cu-Kα radiation (λ=1.5406 Å). Next, the absorption spectra of the samples were determined by Ultraviolet spectroscopy

(UV-Vis, SHIMADZU UV-1800 UV-Visible Series). The measured absorbance wavelength was set to 200nm to 800nm. Lastly, the electrical properties of TiO₂-rGO were obtained by using Keithley Sourcemeter (Model 2450). The measured data from Keithley were presented as current-voltage (I-V) graph.

3. RESULTS AND DISCUSSION

3.1 X-ray Diffraction (XRD)

The X-ray diffraction (XRD) pattern of TiO₂-rGO nanoparticles were obtained at different doping ratio as shown at diffraction peak of $2\theta = 25.3^\circ, 37.9^\circ, 47.9^\circ, 54.0^\circ, 55.3^\circ, 62.5^\circ, 68.9^\circ, 70.5^\circ$ and 75.3° . This can be assigned to (101), (004), (200), (105), (211), (204), (116), (220) and (215) that corresponds to anatase phase of titania agrees with (JCPDS card no: 21-1272) [12; 1]. Figure 2 shows the XRD patterns of TiO₂ and TiO₂-rGO nanocomposites subjected to annealing temperature at 450°C. The characteristics peak of rGO could not be observed due to the minimal volume of rGO to be traced by XRD and it is shadowed by the main peak of anatase TiO₂ at (101) which is consistent with the previous research [13]. In addition, the absence of rGO peak may be due to high crystallinity of TiO₂ [11,14]. It could be observed that the intensity of the diffraction peak is decreasing when the amount of rGO increased. There are no other contamination peaks detected which implies that a high purity of TiO₂ nanoparticles were synthesized as shows in the previous study [8].

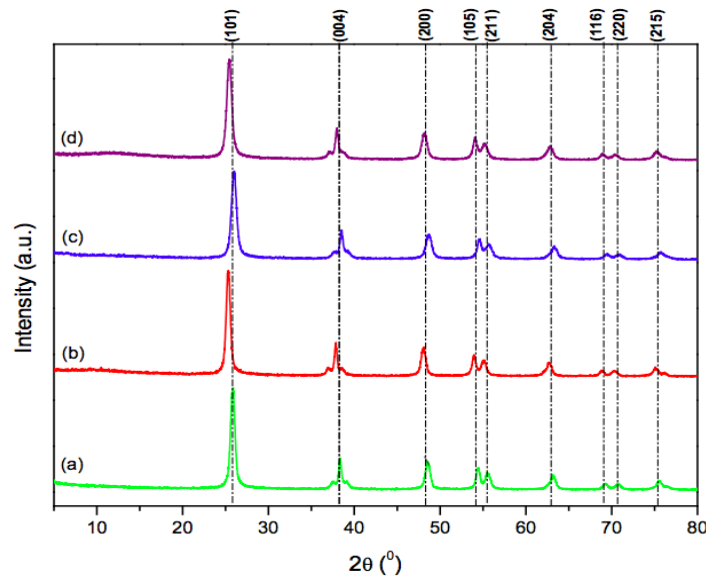


Figure 2. XRD analysis of (a) TiO₂, (b) 0.1wt% TiO₂-rGO, (c) 0.3wt% TiO₂-rGO and (d) 0.5wt% TiO₂-rGO

The average crystalline particle size are calculated by applying Scherer expressions:

$$D = \frac{0.9 \lambda}{\beta \cos(\theta)} \quad (1)$$

where λ is the X-ray wavelength (1.5406 Å-Cu K α radiation), β is the line broadening at half maximum intensity (FWHM) and θ is the Bragg angle. Therefore, the obtained particle size results are shown in Table 2. The 0.1wt% TiO₂-rGO shows the smallest average particle size in relation to the highest crystallinity compared to other samples. Nouri and his team has

reported that the widening of full width at half maximum (FWHM) of the strongest peak at (101) might be due to the smallest crystalline size [15,16]. According to the TiO₂-rGO NC, 0.1wt% TiO₂-rGO is assumed to have the highest intensity which indicates the best crystalline structure causing the decrement in the band gap material.

Table 2 Average particle size of the sample

Sample	2θ (°)	FWHM	Average particle size (nm)
TiO ₂	25.87	0.6071	14.87
0.1wt% TiO ₂ -rGO	26.01	0.7032	12.63
0.3wt% TiO ₂ -rGO	25.32	0.5858	15.12
0.5wt% TiO ₂ -rGO	25.44	0.6926	13.17

3.2 Ultraviolet-visible (UV-Vis) spectroscopy

The comparison for absorbance wavelength of pure TiO₂, 0.1wt% TiO₂-rGO, 0.3wt% TiO₂-rGO and 0.5wt% TiO₂-rGO is shown in Figure 3. It is clearly shown that 0.1wt% TiO₂-rGO is shifted to higher wavelength in the absorbance edge. This will enhance the visible light absorption due to the incorporation of graphene compared to 0.5wt% TiO₂-rGO. This shows that the presence of rGO affects the optical properties of TiO₂-rGO. The decreasing in band gap energy for TiO₂-rGO NC shows a decrease in charge carrier recombination compared to pure TiO₂.

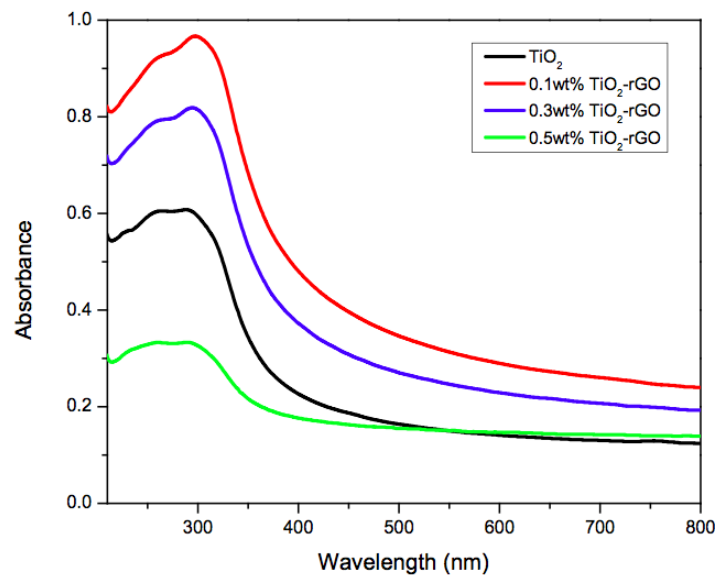


Figure 3. UV-Vis spectroscopy of TiO₂ and different doping ratio of TiO₂-rGO

In order to obtain the band gap, the UV-Vis spectra must be converted into Tauc Plot by using the Kubelka-Munk (K-M) formula as followed:

$$\alpha hv = A(hv - E_g)^2 \quad (2)$$

Where α is absorbance coefficient, h is the plank's constant (4.136×10^{-15} eV), A is the constant (~ 1), v is the speed of light (3×10^8 ms⁻¹), E_g is the band gap energy and n is the

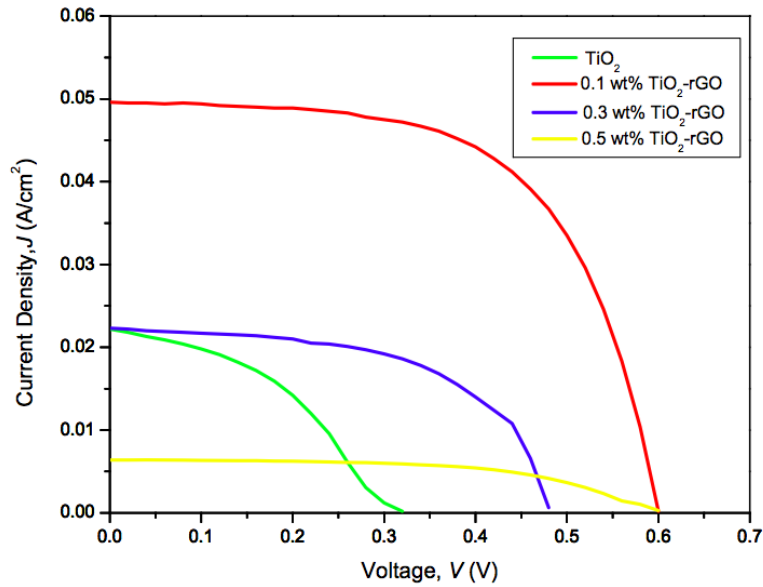
indirect allowed transition (2). Table 3 shows the band gap energy for TiO₂, 0.1wt% TiO₂-rGO, 0.3wt% TiO₂-rGO and 0.5wt% TiO₂-rGO. The 0.1wt% TiO₂-rGO shows the smallest band gap energy of 2.75 eV, respectively. This may be due to the formation of Ti-O-C bond which is formed between Ti⁴⁺ and rGO nanosheets during doping process [15]. The smaller the band gap implies a better formation of Ti-O-C bond between TiO₂ and rGO NC [17].

Table 3 Band gap energy for all samples

Sample	Band Gap Energy (eV)
TiO ₂	3.07
0.1wt% TiO ₂ -rGO	2.75
0.3wt% TiO ₂ -rGO	2.87
0.5wt% TiO ₂ -rGO	2.91

3.3 I-V Plot

The DSSC performance of pure TiO₂ and TiO₂-rGO with different concentration are shown in Figure 4. Table 4 shows the photovoltaic characteristics of DSSC such as short circuit current (J_{sc}), open circuit voltage (V_{oc}), fill factor (FF) and efficiency (η). It can be observed that 0.1wt% TiO₂-rGO achieved highest power conversion efficiency of 1.21% with J_{sc} of 0.049 A/cm², V_{oc} of 0.6 V, and FF of 0.612. The highest V_{oc} obtained might be due to shifting of energy band of TiO₂ that helps the excited electron to reach the conduction band of FTO which results in accumulation of injected electrons [18]. The value of FF of the solar cell indicates the improved of electron life time [19].

**Figure 4.** J-V curve of DSSC

The following are the formula to calculate the fill factor, FF and efficiency, η :

$$\eta = \frac{P_{max}}{P_{in}} = \frac{I_{mp}V_{mp}}{P_{in}} = \frac{I_{sc}V_{oc}FF}{P_{in}} \quad (3)$$

$$FF = \frac{V_{mp}I_{mp}}{I_{sc}V_{oc}} \quad (4)$$

where P_{max} is the maximum power, P_{in} is the input power, I_{mp} is the maximum current, V_{mp} is the maximum voltage, V_{oc} is the open circuit voltage, I_{sc} is the short circuit current and FF is the fill factor. As observed in Table 4, the efficiency of 0.3wt% TiO₂-rGO is still higher than pure TiO₂ but lower than 0.1wt% TiO₂-rGO (1.21%). The initial increase of efficiency is due to the enhancement of electronic conductivity from the increased amount of rGO used in the doping process [20,12]. However, 0.5wt% of TiO₂-rGO has the lowest power conversion efficiency of 0.14% with V_{oc} of 0.6 V, J_{sc} of 0.006 A/cm² and FF of 0.583. This might be due to the excessive amount of rGO which might acts as recombination centers for photo-induced charge carriers that can lead to lower sensitivity of solar simulation [21,22]

Table 4 Photovoltaic characteristics of DSSC

Samples	Short circuit current density, I_{sc}/J_{sc} (A/cm ²)	Open circuit voltage, V_{oc} (V)	Fill factor, FF	Efficiency, %
Pure TiO ₂	0.022	0.320	0.409	0.19
0.1wt% TiO ₂ -rGO	0.049	0.600	0.612	1.21
0.3wt% TiO ₂ -rGO	0.022	0.480	0.547	0.39
0.5wt% TiO ₂ -rGO	0.006	0.600	0.583	0.14

4. CONCLUSION

This research has demonstrated the preparation of TiO₂ and rGO solution for doping process of TiO₂-rGO. The structural, optical and electrical properties of TiO₂-rGO are fully characterized. The structural properties of TiO₂-rGO indicates that the doping of rGO maintain the crystallinity structure of anatase TiO₂. For optical properties, the doping of rGO enhances the photocatalytic activity by reducing the band gap of TiO₂-rGO. This can be proved by 0.1wt% TiO₂-rGO shows the smaller band gap of 2.75 eV compared to pure TiO₂, 3.07 eV. 0.1wt% TiO₂-rGO shows the ideal sample acts as photoanode in DSSC which resulting in highest electrical properties in this research.

ACKNOWLEDGEMENT

The authors gratefully acknowledge the Ministry of Higher Education for Fundamentals Research Grant Scheme (FRGS) F02/FRGS/1617/2017 and Universiti Malaysia Sarawak (UNIMAS) for their kind support and encouragement through this research.

REFERENCES

- [1] F. W. Low, C. W. Lai & S. B. Abd Hamid, "Study of reduced graphene oxide film incorporated of TiO₂ species for efficient visible light driven dye-sensitized solar cell," *Journal of Material Science*, **28**, (2017) 3819-3836.
- [2] S. K. Sahari, M. Sawawi, M. Kashif, A. Baharin, R. Kemat & E. Jaafar, "Sensitization of TiO₂ Thin Film with Different Dye for Solar Cell Application," *Journal of Telecommunication, Electronic and Computer Engineering (JTEC)*, **9**, 3-10 (2017) 49-52.

- [3] J. Sheng et al., "Characteristics of dye-sensitized solar cells based on the TiO₂ nanotube/nanoparticle composite electrodes," *Journal of Material Chemistry*, **21**, 14 (2011) 5457-5463.
- [4] Y. S. Jin et al., "The effect of RF-sputtered TiO₂ passivating layer on the performance of dye sensitized solar cells," *Ceramics International*, **38**, (2012) S505-S509.
- [5] A. N. B. Zulkifli, T. Kento, M. Daiki & A. Fujiki, "The Basic Research on the Dye-Sensitized Solar Cell," **3**, 5 (2014) 382-388.
- [6] A. Eshaghi & A. A. Aghaei, "Effect of TiO₂-graphene nanocomposite photoanode on dye-sensitized solar cell performance," *Bulletin of Material Science*, **38**, 5 (2015) 1177-1182.
- [7] F. W. Low & C. W. Lai, "Recent development of graphene-TiO₂ composite nanomaterials as efficient photoelectrodes in dye-sensitized solar cells," *Renewable and Sustainable Energy Reviews*, **82**, (2018) 103-125.
- [8] F. W. Low & C. W. Lai, "Reduced Graphene Oxide decorated TiO₂ for Improving Dye-Sensitized Solar Cells (DSSCs)," *Current Nanoscience*, **14**, (2018) 1-6.
- [9] F. W. Low, C. W. Lai & S. B. Hamid, "One-step Hydrothermal synthesis of titanium dioxide decorated on reduced graphene oxide for dye sensitized solar cells application," *International Journal of Nanotechnology*, **15**, 1/2/3 (2018) 78-92.
- [10] F. W. Low, C. W. Lai & S. B. Hamid, S. Chong & W. W. Liu, "High Yield Preparation of Graphene Oxide Film Using Improved Hummer's Technique for Current-Voltage Characteristics," *Advanced Material Research*, **1109**, (2015) 385-389.
- [11] C. W. Lai, F. W. Low, S. W. Chong, C. P. Wong, S. Z. Siddick, C. J. Juan & S. B. Hamid, "An Overview: Recent Development of Titanium Dioxide Loaded Graphene Nanocomposite Film for Solar Application," *Current Organic Chemistry*, **19**, 19 (2015) 1882-1895.
- [12] J. Zhang, Z. Xiong & X. S. Zhao, "Graphene-metal-oxide composites for the degradation of dyes under visible light irradiation," *Journal of Materials Chemistry*, **21**, 11 (2011) 3634-3640.
- [13] H. Ding, S. Zhang, J. T. Chen, X. P. Hu, Z. F. Du, Y. X. Qiu & D. L. Zhao, "Reduction of graphene oxide at room temperature with vitamin C for rGO-TiO₂ photoanodes in dye sensitized solar cell," *Thin Solid Films*, **584**, (2015) 29-36.
- [14] J. S. Lee, K. H. You & C. B. Park, "Highly proactive, low bandgap TiO₂, nanoparticles wrapped by graphene," *Advanced Materials*, **24**, (2012) 1084-1088.
- [15] F. W. Low, C. W. Lai, K. M. Lee & J. C. Juan, "Enhance of TiO₂ dopants incorporated reduced graphene oxide via RF magnetron sputtering for efficient dye-sensitized solar cells," *Rare Metals*, **37**, 11 (2018) 919-928.
- [16] E. Nouri, M. Reza & P. Lianos, "Impact of preparation method of TiO₂-rGO nanocomposite photoanodes on the performance of dye-sensitized solar cells," *Electrochimica Acta*, **219**, (2016) 38-48.

- [17] H. Awang & N. I. Talahah, "Synthesis of Reduced Graphene Oxide-Titanium (rGO-TiO₂) Composite Using a Solvothermal and Hydrothermal Methods and Characterized via XRD and UV-Vis," *Natural Resources*, **10**, 2 (2019) 17-28.
- [18] H. Elbony, A. Thapa, P. Poudel, N. Adhikary, S. Venkatesan & Q. Qiao, "Vanadium Oxide as a new charge recombination blocking layer for high efficiency dye-sensitized solar cells," *Nano Energy*, **13**, (2015) 368-375.
- [19] R. Raja, M. Govindaraj, M. D. Antony, K. Krishnan, E. Velusamy, A. Sambandam, V. W. Rayar, "Effects of TiO₂/rGO composite thin film as a blocking layer on the efficiency of dye-sensitized solar cells," *Journal of Solid State Electrochemistry*, **21**, 3 (2016) 891-903.
- [20] B. Tang, H. Chen, H. Peng, Z. Wang & W. Huang, "Graphene Modified TiO₂ Composite Photocatalysts: Mechanism, Progress and Perspective," *Nanomaterials*, **8**, 2 (2018) 105.
- [21] Y. Zhang & C. Pan, "TiO₂/Graphene composite from thermal reaction of graphene oxide and its photocatalytic activity in visible light," *Journal of Materials Science*, **46**, 8 (2010) 2622-2626.
- [22] M. R. Hasan, S. B. Hamid, W. J. Basirun, S. H. M. Suhaimy & A. N. Che Mat, "A sol-gel derived, copper dioxide-reduced graphene oxide nanocomposite electrode for the photoelectrocatalytic reduction of CO₂ to methanol and formic acid," *Royal Society of Chemistry*, **5**, (2015) 77803-77813.